8-2009

Continued Development of an Empirical Function for Predicting and Rationalizing Protein–Protein Binding Affinities

Joseph Audie
Sacred Heart University

Recommended Citation

Audie, J. (2009). Continued development of an empirical function for predicting and rationalizing protein–protein binding affinities. *Biophysical Chemistry, 143*(3), 139-144. Doi: 10.1016/j.bpc.2009.05.003

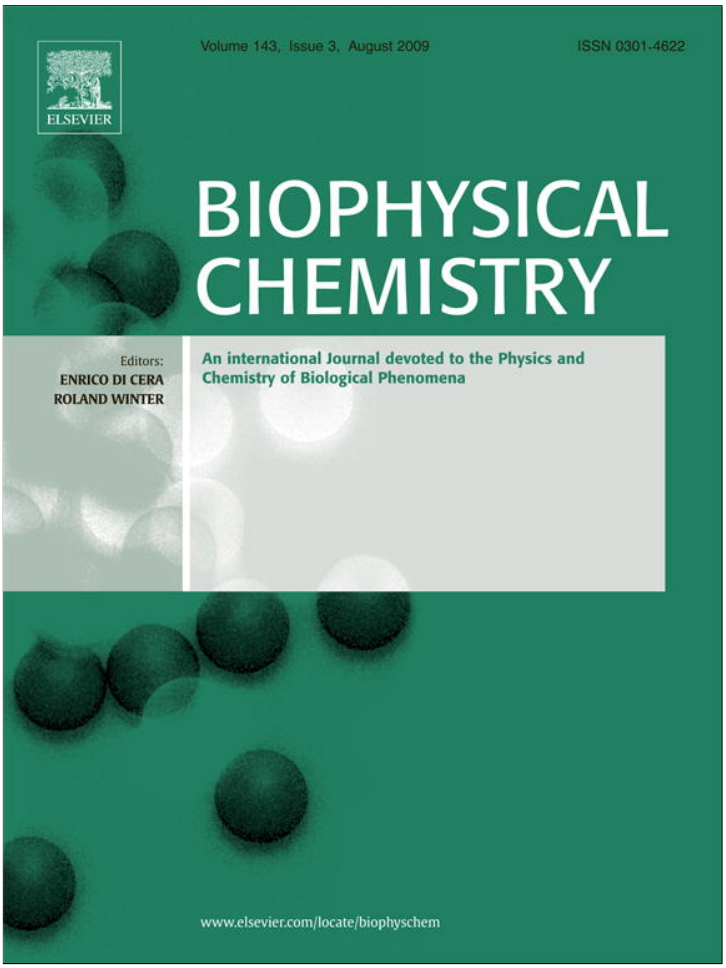

Biophysical Chemistry 143 (2009) 139–144

Contents lists available at ScienceDirect

Biophysical Chemistry

journal homepage: http://www.elsevier.com/locate/biophyschem

Continued development of an empirical function for predicting and rationalizing protein–protein binding affinities

Joseph Audie *

Department of Chemistry, Sacred Heart University, Fairfield, CT 06825, United States
CMD Bioscience, Orange, CT, United States

ARTICLE INFO

Article history:
Received 11 March 2009
Received in revised form 8 May 2009
Accepted 11 May 2009
Available online 14 May 2009

Keywords:
Protein–protein recognition
Binding affinity
Free energy
Alanine scanning mutagenesis
Hot spot
Peptide therapeutics
Biologics
Computational

ABSTRACT

Here we summarize recent work on the continued development of our fast and simple empirical equation for predicting and structurally rationalizing protein–protein and protein–peptide binding affinities. Our empirical expression consists of six regression-weighted physical descriptors and derives from two key simplifying assumptions: (1) the assumption of rigid-body association and (2) the assumption that all contributions not explicitly considered in the equation make a net contribution to binding of ≈0 kcal. Within the strict framework of rigid-body association, we tested relative binding affinity predictions using our empirical equation against the corresponding experimental binding free energy data for 197 interface alanine mutants. Our methodology produced excellent agreement between prediction and experiment for 79% of the mutations considered. These encouraging results further suggest the basic validity of our approach. Further analysis suggests that the majority of the failed predictions can be accounted for in terms of mutation induced violations of assumption (2). In particular, we hypothesize that assumed away charge and aromatic side chain-mediated electrostatic interface interactions play a key role in protein–protein recognition and that such interactions must be explicitly considered for a more generally valid approach to physics-based binding affinity prediction.

1. Introduction

Protein interaction networks are essential to life. Thus, a quantitative understanding of what physical factors drive and modulate protein–protein association is of obvious importance. Indeed, a considerable amount of recent work has been done researching free energy methods for predicting and structurally rationalizing protein–protein binding affinities[1–4]. Likewise, the development of protein and peptide based therapeutics and the successful implementation of structure based drug design projects aimed at regulating protein–protein interactions would be aided by the development of improved quantitative methods for predicting and explaining the thermodynamics, specificity and physical basis of protein–protein recognition [5–12].

We have previously described a six-term, regression-weighted, empirical free energy function that was used to predict experimental binding free energies for a large and diverse number of native protein–protein and protein–peptide interactions to within ≈1.0 kcal. Moreover, we argued that the function and its various physical descriptors were in basic agreement with theory and experiment. As such, we tentatively concluded that our empirical equation explicitly captured at least some of the underlying physics of protein–protein recognition. It is important to note, however, that the function derives from two key simplifying assumptions: (1) the assumption of rigid-body association and (2) the assumption that neglected interface interactions, in particular neglected electrostatic interactions, combine to offset the desolvation penalties that are not explicitly accounted for in our empirical expression [13].

More recently, we tested the function for its ability to correctly score and rank native and non-native protein–protein binding modes that were generated using the Hex rigid-body protein–protein docking server (http://www.csd.abdn.ac.uk/hex_server/) [14]. The function performed surprisingly well but only after it was modified to energetically penalize solvent exposed hydrogen bonding interactions, suggesting an important role for previously neglected or unaccounted for electrostatic interactions. Even this modification, however, failed to produce physically realistic free energy surfaces for all of the tested protein–protein interactions [15]. A possible explanation is that assumption (2) breaks down in the case non-native interactions or that assumption (2) is only reasonable for interfaces that are characterized by sufficiently buried and sufficiently complimentary electrostatic interactions. Thus, our previous work suggests that assumption (2) provides a reasonable and useful approximation in the case of native protein–protein interactions but that it breaks down in the case of non-native interactions. Hence, the

* Department of Chemistry, Sacred Heart University, Fairfield, CT 06825, United States.
E-mail address: audiej@sacredheart.edu.

0301-4622/$ – see front matter © 2009 Elsevier B.V. All rights reserved.
doi:10.1016/j.bpc.2009.05.003

successful prediction of non-native binding affinities would seem to require the explicit consideration of energetic contributions, in particular electrostatic contributions, which are currently neglected in our six-term free energy expression.

To facilitate the development of our empirical methodology into a more robust and more generally valid computational binding free energy prediction method we decided to test its performance against a large and diverse test set of 197 protein–protein wild-type (wt) and alanine (Ala) mutants (mut) and their associated and experimentally (exp) determined relative binding free energies ($\Delta\Delta G_{exp,mut-wt} = \Delta G_{exp,mut} - \Delta G_{exp,wt}$). Single Ala interface mutants would seem to provide good test cases for evaluating and further developing our binding free energy methodology. First, recent computational work and *a priori* physical reasoning indicate that the vast majority of isolated Ala mutants can be accounted for by assuming rigid-body association [16–18]. Second, single Ala substitutions represent targeted and relatively undisruptive interface events. These two considerations suggested that we would be able to successfully predict a majority of the $\Delta\Delta G_{exp,mut-wt}$ values and that we would also be able to focus in on the neglected interface interactions that might explain any (anticipated) predictive failures.

In sum, we tested our six-term empirical binding free energy function against a large and diverse test set of 197 Ala mutants. In keeping with our prior expectations, we were able to successfully predict relative binding affinities for fully 79% of the 197 Ala mutations studied to within ≈1.2 kcal. This encouraging result further suggests the basic usefulness and validity of our methodology. The function failed to generate good predictions for a relatively high percentage of charged and aromatic residue alanine substitutions. This result suggests something peculiar about charged and aromatic side chain interactions that are neglected by our approach.

A possible explanation for the observed pattern of predictive successes and failures is that assumption (2) is sometimes violated following an alanine substitution for charged and aromatic side chains or that various charge-group and aromatic-group (π) mediated electrostatic interactions must be explicitly quantified for a binding free energy expression to qualify as generally valid and that our empirical equation should be modified accordingly. Importantly, this inference is in good agreement with our previous work on the prediction of native and non-native binding affinities and also seems to be in good agreement with independent work that suggests an important role for electrostatic interactions in protein–protein hot spot prediction [17,18]. Ultimately, the present study helps to further elucidate the physical basis of protein–protein recognition and suggests new research avenues for our continued efforts at developing a fast, quantitative, physics-based and generally accurate method for protein–protein binding free energy prediction and rationalization.

2. Methods

The goal of the present study was to test our empirical equation for predicting and rationalizing protein–protein binding stability changes against a test set of protein–protein Ala mutants. For the purposes of this paper, rigid-body association is defined as the total absence of any conformational rearrangements of either the bound or unbound states following the computationally engineered truncation of a given wt type residue to alanine. By implication, all free energy predictions were made from either static wt complex crystal structures or from mutant complex structures following mere alanine truncation.

Firstly, binding affinities ($\Delta G_{bind,wt}$) were calculated from the coordinates of the various crystallographic wt complex structures employed in the study, assuming rigid-body association. Secondly, interface alanine mutations were introduced into the various complex structures by a simple side chain truncation procedure and no additional structural optimization was performed either before or after the truncation to alanine. Thirdly, binding affinities were calculated for all alanine mutants ($\Delta G_{bind,mut}$), assuming rigid-body association. Finally, relative binding affinities were calculated ($\Delta\Delta G_{bind,wt-mut} = \Delta G_{bind,mut} - \Delta G_{bind,wt}$) and analyzed against experimental relative binding affinity data ($\Delta\Delta G_{exp,wt-mut}$).

2.1. Theory

2.1.1. The binding free energy

Assuming rigid-body association and starting from a given wt or mutant protein–protein coordinate file, the binding free energy (ΔG_{bind}) can be calculated from a linear combination of six regression-weighted physical descriptors,

$$\Delta G_{bind} = -0.79\Delta X_{+/-} + 0.075\Delta X_{c/s} - 0.65X_{sb} - 0.86X_{hb} - 0.00089X_{gap} - 0.089\Delta X_{tor} - 0.33 \quad (1)$$

where the first two terms refer to changes in the total number of solvent exposed charged and apolar atoms, respectively. The third and fourth terms refer to the net number (difference between favorable and unfavorable charge–charge contacts) of short range (≤4 Å) charge–charge or salt bridge interactions across the protein–protein interface and the total number of interface hydrogen bonds. The final two terms, in order, refer to the interface gap or void volume and the change in the number of solvent exposed side chain torsions or "free" side chain torsions following complex formation. All parameters and definitions are taken from our previous papers [13,15].

According to our current physical interpretation, the first term in Eq. (1) relates to the free energy cost of rupturing hydrogen bonds between charged atoms and water and the second term gives the favorable solvent entropy change that accompanies apolar group burial (hydrophobic effect). The third and fourth terms, in order, give the net electrostatic free energy contribution of interchain salt bridge interactions and the quantum mechanical (QM) or quasi-covalent energy of interchain hydrogen bonding interactions. The fifth term estimates the free energy contribution of water-bridged protein–protein interactions and the sixth term gives the conformational entropy change [13].

Following an $X \rightarrow$ Ala mutation, where X refers to one of the 20 standard amino acids, the relative binding free energy ($\Delta\Delta G_{bind,wt-mut} = \Delta G_{bind,mut} - \Delta G_{bind,wt}$) is given by,

$$\Delta\Delta G_{bind,wt-mut} = -0.79\Delta\Delta X_{+/-} + 0.075\Delta\Delta X_{c/s} - 0.65\Delta X_{sb} - 0.86\Delta X_{hb} - 0.00089\Delta X_{gap} - 0.089\Delta\Delta X_{tor} \quad (2)$$

The only difference between Eqs. (1) and (2) is that $\Delta\Delta G_{bind,wt-mut}$ is predicted from relative changes in wt and mut descriptor values. Clearly, and as discussed in the introduction, numerous interactions are ignored or assumed away in Eqs. (1) and (2). In particular, Eqs. (1) and (2) fail to explicitly treat the electrostatic free energy contribution to binding associated with the formation of interchain polar-charge contacts, π–π contacts, cation–π contacts and long range charge–charge interactions.

2.2. Computational details

2.2.1. Calculating the binding free energy

All predicted binding affinities were calculated using Eq. (1) as implemented by our Affinity empirical free energy function. The function generates binding affinity predictions from a single, static, protein–protein complex input coordinate file and has an accuracy of ≈1.0 kcal. The Affinity function is available from CMD Bioscience (www.cmdbioscience.com) and, in the interest of full disclosure, it should be pointed out that the author of the present paper is a co-founder of the company.

Since first describing our empirical methodology for binding affinity estimation we have (1) re-optimized the function on an improved training set, (2) added an explicit term for interface clash detection and (3) introduced a procedure for grading the energetic contributions of hydrogen bonds and salt bridges according to the average solvent accessible surface area (SASA) of the interacting atoms. In the present study the clash term was omitted, since all structures lacked interface clashes and truncation to alanine can never result in new steric clashes. The magnitude of the charge–charge contribution goes to zero when the average SASA of a charged atom pair exceeds a user-defined threshold (25.9 Å^2). Likewise, the user can independently penalize polar–polar and charge–polar hydrogen bonds according to the total average SASA of the hydrogen bonds (8.0 and 17.0 Å^2, respectively). The default SASA values employed in the present study were derived from an analysis of our training and test sets and have been shown to work well for estimating native and non-native binding affinities [15].

In practice Eq. (1) was used to calculate $\Delta G_{bind,wt}$ and $\Delta G_{bind,mut}$, assuming rigid-body association. From these individual binding affinity predictions, we calculated $\Delta\Delta G_{bind,wt-mut}$ values. The entire process is quantitatively summarized by Eq. (2). All parameters and values employed in the present study are default ones.

2.2.2. Wild type and alanine mutant structures

Candidate protein–protein complex structures, alanine mutant sequence positions and $\Delta\Delta G_{exp,wt-mut}$ values were obtained from the literature and from the Alanine Scanning Energetics Database (ASEdb) (http://nic.ucsf.edu/asedb/index.php) [19,20]. All crystallographic complex structures were downloaded from the Protein Data Bank (PDB) (http://www.rcsb.org/pdb/home/home.do). Complexes employed in the study included 1a4y, 1ahw, 1brs, 1bxi, 1cbw, 1fcc, 1gc1, 1vfb, and 3hhr (see Table 1). Only residues with an atom within 10 Å of an atom from an interacting chain were modeled in the study, as 10 Å is the longest range interaction calculated in Eq. (2) (the gap volume descriptor); the molecular visualization and modeling program Deep View was used to identify all such residues (http://spdbv.vital-it.ch/); a total of 197 alanine mutations were explicitly modeled and analyzed.

2.2.3. Generating the alanine mutants

Starting from a given wt complex structure, $X \rightarrow$ Ala substitutions were introduced at select residue positions through a simple truncation procedure using the side chain modeling program SCCOMP (http://ignmtest.ccbb.pitt.edu/cgi-bin/sccomp/sccomp1.cgi). In an effort to keep things as simple as possible, only SCCOMP default parameters were employed and no additional structural optimization was performed. This mutation procedure minimizes computational costs and rigorously ensures the assumption of rigid-body association. Following the construction of the alanine mutants, relative binding free energy changes were calculated for all wt and mutant structures according to Eq. (2) (see Suppl information).

2.2.4. Comparing computational predictions with experimental data

Experimental relative binding free energy data ($\Delta\Delta G_{exp,wt-mut}$) was obtained from the ASEdb database and from the literature. Predicted relative binding free energies were calculated from the formulae $\Delta\Delta G_{bind,wt-mut} = \Delta G_{bind,mut} - \Delta G_{bind,wt}$ according to Eq. (2). For a given mutant, a prediction was counted as accurate for $|\Delta\Delta G_{bind,wt-mut} - \Delta\Delta G_{exp,wt-mut}| \leq 1.2$ kcal, which is consistent with the known error of Eq. (1) and roughly equates with chemical accuracy [18].

3. Results

PDB codes and interaction types for the nine protein–protein complexes used in the study are presented in Table 1. Relative binding affinities ($\Delta\Delta G_{bind,wt-mut}$) were calculated from all 9 wt complexes for a total of 197 alanine mutant structures according to Eq. (2). $\Delta\Delta G_{bind,wt-mut}$ values were then compared with their corresponding experimental values ($\Delta\Delta G_{exp,wt-mut}$). A prediction was counted as successful when it was found that $|\Delta\Delta G_{bind,wt-mut} - \Delta\Delta G_{exp,wt-mut}| \leq 1.2$ kcal. This data was then used to calculate relative binding affinity prediction success rates. The overall root-mean-squared deviation for all successful predictions (155 data points) is also given in Table 1 (0.56 kcal). The average unsigned error is also provided in Table 1 (0.46 kcal). The RMSD error and average unsigned error for all 197 mutants is 1.3 kcal and 0.88 kcal, respectively. As can be seen from Table 1, success rates ranged from a high of 94% (1gc1) to

Table 1
Alanine mutants and overall relative binding affinity prediction success rates.

PDB[a]	Mutated protein[b]	Partner protein[c]	Total mutations[d]	Predicted mutations[e]	Successful predictions[f]	Success rate[g]
1a4y	Angiogenin	Rnase inhibitor	14	14	12	86%
1a4y	Rnase inhibitor	Angiogenin	14	14	9	64%
1ahw	Tissue Factor	Fab 5G9	8	8	7	88%
1brs	Barnase	Barstar	8	8	2	25%
1brs	Barstar	Barnase	6	6	4	67%
1bxi	1 m9	E9 Dnase	28	28	24	86%
1cbw	BPTI	Chymotrypsin	9	9	8	89%
1fcc	B1 domain	Human fc	8	8	4	50%
1gc1	CD4	gp120	49	31	28	94%
1vfb	HEL	D1.3	17	12	10	83%
3hhr	hGH	hGhbp,site1	31	31	24	81%
3hhr	hGH	hGhbp,site?	31	28	23	86%
Overall values			223	197	155	79%
					RMSD Error[h]	0.56 kcal (0.46 kcal)

A total of 9 protein–protein complexes and 197 $X \rightarrow$ Ala mutations were studied. Experimental relative binding free ($\Delta\Delta G_{exp,wt-mut}$) energies were obtained from the ASEdb database and the literature (see text). Predicted relative binding affinities ($\Delta\Delta G_{bind,wt-mut}$) were then calculated for all 197 mutants using Eqs. (1) and (2). A prediction for a given $X \rightarrow$ Ala mutation was counted as successful if $\Delta\Delta G_{bind,wt-mut}$ was within 1.2 kcal of $\Delta\Delta G_{exp,wt-mut}$. From this data, prediction success rates were calculated for each complex by dividing the number of successful predictions by the total number of predictions. An RMSD error for all predictions was also calculated (0.56 kcal).

[a] Protein data bank (PDB) codes for all protein dimer complexes used in the present study.

[b] Protein monomer with residues mutated to alanine.

[c] Protein monomer that served as un-mutated (wt) partner protein.

[d] Total interface alanine mutations reported and considered for each protein–protein complex.

[e] Total number of alanine mutations actually modeled and studied; alanine substitutions on a given monomer chain were modeled only if they were within 10 Å of the other monomer chain; binding free energy predictions ($\Delta\Delta G_{bind,wt-mut}$) were only attempted for these mutations.

[f] $\Delta\Delta G_{bind,wt-mut}$ values were counted as successful if they were within 1.2 kcal of $\Delta\Delta G_{exp,wt-mut}$.

[g] Successful predictions/predicted mutations.

[h] Root-mean-squared deviation (in kcal) for all successfully predicted $\Delta\Delta G_{bind,wt-mut}$ values; average unsigned error is provided in parentheses.

a low of 25% (1brs) with an overall success rate of ≈79% for all 197 mutants studied (155 / 197).

All of the 19 non-alanine standard amino acid residues are represented among the 197 alanine mutations studied. To try and elucidate the physical basis for the successful and unsuccessful predictions made using Eq. (2), prediction success rates were calculated on a residue basis and the data is provided in Table 2. With the exception of Trp and Tyr, all other residues were predicted quite well. It is also worth noting that Arg and Lys displayed lower success rates than the other amino acids. Residues were also grouped according to the physical properties of the side chain, particularly according to side chain charge, hydrogen bonding potential and aromaticity. Charged side chains include D, E, K and R. Apolar residues include C, I, L, M, V, G and P. Polar side chains include T, S, Q, N, and H. Aromatic residues included F, W and Y. Given these classifications, prediction success rates were calculated for charged (73%), polar (89%), apolar (85%) and aromatic residues (50%).

In an effort to gain further insight into the physical reasons for our failed predictions, information regarding the failed predictions was tabulated and is presented in Table 3. Eq. (2) failed to produce accurate $\Delta\Delta G_{\mathrm{bind,wt-mut}}$ predictions for 42 $X \rightarrow$ Ala mutations, where X is a charged, polar, aromatic or apolar residue. Of the 42 residues, 40 could be clearly classified as interface residues (within 5 Å of an interacting chain); two residue side chains (Ile 58 (3hhr) and Asn 58 (1brs)) occupy positions far removed from their respective interfaces and thus probably impact binding through monomer destabilization and are omitted from further discussion.

Three failed predictions (1gc1 Q40A, 3hhr H18A, and 3hhr E174A) involve experimentally determined relative binding affinity changes less than zero ($\Delta\Delta G_{\mathrm{exp,wt-mut}}<0$) and all are very close to experimental error. Interestingly, for five of the mutant test cases (1bxi E30A, 1fcc K28A, 1gc1 R59A, 3hhr N12A, and 3hhr R16A) the magnitude of the predicted destabilization ($\Delta\Delta G_{\mathrm{bind,wt-mut}}$) exceeds the experimentally determined level of complex destabilization ($\Delta\Delta G_{\mathrm{exp,wt-mut}}$). This suggests that conformational rearrangement at the interface can mitigate the destabilizing effects of lost stabilizing interchain contacts and that our methodology should be modified accordingly. A detailed discussion of this possibility, however, is beyond the scope of the present study. Hence, these results are ignored in the analysis and discussion that follows.

The guiding assumption of this paper, to be discussed in what follows, is that the remaining 32 failed predictions can probably be accounted for in terms of interface interactions that are lost following truncation to Alanine and that are neglected in Eqs. (1) and (2). Of the 32 remaining failed predictions, 16 involve charged residues, 9 involve aromatic residues, 3 involve polar residues and 4 involve apolar residues. The RMSD error is ≈3.0 kcal, 2.30 kcal, 2.0 kcal and 1.2 kcal for the charged, aromatic, apolar and polar residue predictions, respectively. The RMSD for all 32 failed predictions is ≈2.8 kcal.

Table 2
Success rate trends for amino acids.

Amino acids	Number of successful predictions	Number of unsuccessful predictions	Total number of predictions	Success rate
C	2	0	2	1.00
D	14	3	17	0.82
E	17	6	23	0.74
F	3	1	4	0.75
G	2	0	2	1.00
H	6	2	8	0.75
I	5	1	6	0.83
K	10	5	15	0.67
L	7	2	9	0.78
M	1	0	1	1.00
N	12	2	14	0.86
P	7	0	7	1.00
Q	11	2	13	0.85
R	15	7	22	0.68
S	19	0	19	1.00
T	12	1	13	0.92
V	6	2	8	0.75
W	2	4	6	0.33
Y	4	4	8	0.50
Charged	56	21	77	0.73
Polar	60	7	67	0.89
Apolar	30	5	35	0.86
Aromatic	9	9	18	0.50

A total of 197 $X \rightarrow$ Ala mutations were studied from 9 protein–protein interactions. On an X residue basis, predicted relative binding free energies ($\Delta\Delta G_{\mathrm{bind,wt-mut}}$) were calculated using Eq. (2) and compared with experimental relative binding free energies ($\Delta\Delta G_{\mathrm{exp,wt-mut}}$). For a given residue type, a calculated $\Delta\Delta G_{\mathrm{bind,wt-mut}}$ was counted as accurate if it was within 1.2 kcal of the corresponding $\Delta\Delta G_{\mathrm{exp,wt-mut}}$ value. Prediction success rates were counted for each residue type by dividing the number of successful predictions by the total number of attempted predictions. Residues were then grouped according to their physical properties. Charged side chains include D, E, K and R. Apolar residues include C, I, L, M, V, G and P. Polar side chains include T, S, Q, N, and H. Finally, aromatic residues include F, W and Y. Based on this classificatory scheme, side chain type success rates were calculated.

Table 3
Failed predictions using Eq. (2) according to complex type, residue type and residue position.

PDB	Residue type	Residue position	$\Delta\Delta G_{\mathrm{exp,wt-mut}}$	$\Delta\Delta G_{\mathrm{bind,wt-mut}}$	Error
1a4y	R	5	2.3	0.3	2.0
1a4y	W	89	0.2	−1.2	1.4
1a4y	W	318	1.5	−0.2	1.7
1a4y	W	375	1.0	−0.7	1.7
1a4y	E	401	0.9	−0.6	1.5
1a4y	Y	434	3.3	0.8	2.5
1a4y	D	435	3.5	1.0	2.5
1ahw	Y	156	4.0	1.0	3.0
1brs	K	27	5.4	0.0	5.4
1brs	N	58	3.1	0.0	3.1
1brs	R	59	5.2	2.1	3.1
1brs	E	73	2.8	−0.7	3.5
1brs	R	87	5.5	2.7	2.8
1brs	H	102	6.0	0.6	5.4
1brs	Y	29	3.4	−0.6	4.0
1brs	D	35	4.5	1.4	3.1
1bxi	E	30	1.4	4.4	3.0
1bxi	L	33	3.4	1.2	2.2
1bxi	D	51	5.9	0.8	5.1
1bxi	V	34	2.6	0.9	1.7
1cbw	K	15	2.0	0.3	1.7
1fcc	E	27	5.0	1.3	3.7
1fcc	K	28	1.3	3.6	2.3
1fcc	K	31	3.5	0.7	2.8
1fcc	W	43	3.8	1.7	2.1
1gc1	E	85	1.3	−0.8	2.1
1gc1	R	59	1.2	2.8	1.6
1gc1	Q	40	−0.4	0.9	1.3
1vfb	V	120	0.9	−0.8	1.7
1vfb	R	125	1.8	−0.7	2.5
3hhr	Q	68	0.6	−1.0	1.6
3hhr	Y	164	0.3	−1.4	1.7
3hhr	K	172	2.0	0.0	2.0
3hhr	E	174	−0.9	0.9	1.8
3hhr	T	175	2.0	0.2	1.8
3hhr	F	176	1.9	0.5	1.4
3hhr	H	18	−0.5	0.8	1.3
3hhr	N	12	0.1	2.1	2.0
3hhr	L	15	0.2	−2.3	2.5
3hhr	I	58	1.6	0.0	1.6
3hhr	R	16	0.2	1.8	1.6
3hhr	R	8	0.2	−1.1	1.3

All columns, terms and quantities are defined and explained in Tables 1 and 2 and in the text.

4. Discussion

The primary purpose of our study was to test and evaluate Eqs. (1) and (2) for estimating the effects of $X \rightarrow$ Ala mutations on protein–

protein binding free energies. It is important to recall that Eqs. (1) and (2) derive from two key simplifying assumptions. Assumption (1) is the assumption of rigid-body association and assumption (2) is the assumption that all contributions not explicitly considered in Eqs. (1) and (2) offset to make a roughly zero net contribution to the free energy of binding.

In an effort to minimize computational cost, to ensure the rigid-body approximation, and to maximize the interpretability of our results in light of assumption (2), we employed the simplest alanine mutation strategy possible: simple side chain truncation with no prior or posterior dynamic structural alteration of any kind for either unbound or bound structures. Importantly, other groups have reported good results using a similar rigid-body approach [16–18].

Relative binding free energy values ($\Delta\Delta G_{\mathrm{bind,wt-mut}}$) were then calculated using the simplest quantitative free energy expression that we are aware of, our own Affinity empirical free energy function (Eqs.(1) and (2)). Importantly, Eq. (2) was not tweaked or re-parameterized for mutation prediction. Thus, if not the theoretically simplest model possible, our alanine mutation model seems to qualify as the simplest one tested to date and can serve as a reference point for research on the problem. Ultimately, this minimalist approach allowed us to better focus our analysis but at the expense of a detailed consideration of some 10 alanine mutant complexes that appear to involve non-trivial conformational remodeling of the bound and/or unbound states.

4.1. Analysis of predictive successes

The overall predictive performance of our model is remarkably good. Fully 79% of all attempted predictions (155/197) are within chemical accuracy (≈1.2 kcal) and with an RMSD error of 0.56 kcal and an average unsigned error of 0.46 kcal. Moreover, with the lone exception of the Barnase (1brs) mutants all complex $\Delta\Delta G_{\mathrm{bind,mut-wt}}$ success rates ranged from satisfactory (1fcc, 50%) to excellent (1gc1, 94%), with the majority of predictions clearly qualifying as very good (≈80%). Finally, with the exceptions of the Tyr and Trp substitutions, Eq. (2) was used to successfully predict relative binding free energies for clear majorities of the remaining residues. These results show that our simple model, as quantitatively summarized in Eq. (2), can satisfactorily account for the binding of a diverse set of randomly selected and disparate protein–protein interactions that have been perturbed by alanine mutagenesis. This, in turn, strengthens our confidence in the basic validity of our approach and further suggests that Eqs. (1) and (2) capture much of the underlying physics of protein–protein recognition.

In summary, for ≈79% of the 197 mutations studied the exclusive use of Eq. (2) proved adequate to predict the effects of Ala mutations on relative binding free energies to within ≈1.2 kcal. Thus, according to our thermodynamic interpretation of Eq. (2) ≈79% of Ala induced relative binding free energy changes can be explained in terms of relative changes in the hydrogen bonding component of the charge group desolvation penalty, relative changes in solvent entropy effects due to apolar group burial, relative changes in interchain salt bridge and hydrogen bonding interactions, relative changes in water-bridged interface interactions, and relative changes in the conformational entropy penalty associated with side chain torsion burial. Put differently, the combination of simplifying assumptions (1) and (2) and six relatively coarse-grained physics-based descriptors suffice to account for ≈79% of the 197 mutations studied.

4.2. Analysis of predictive failures

We obtained a total of 42 predictive failures. Our results suggest that 10 of these involve mechanisms beyond the truncation induced loss of interface interactions; these predictive failures probably require explanation with reference to assumptions (1) and (2) and will not be considered further. The remaining 32 predictive failures can probably be accounted for in terms of violations of assumption (2).

Even a cursory look at the data regarding the nature and magnitudes of the 32 predictive failures paints an unavoidably clear picture: the primary shortcoming of Eqs. (1) and (2) has to do with an inadequate treatment of charged and aromatic side chains. Indeed, if the imidazole ring of His is included, fully 81% (26/32) of the failed predictions involve charged or aromatic side chain substitutions with an RMSD of ≈2.8 kcal. Therefore, we think it is reasonable and will prove most profitable to focus our attention on these 26 charged and aromatic residue side chains for the remainder of the paper.

The 26 charged and aromatic residue mutations we failed to predict entail relative complex destabilizations ($\Delta\Delta G_{\mathrm{exp,wt-mut}}$) which, at least in theory, can be explained by mutation induced monomer destabilization (assumption (1)) or through the mutation induced loss of stabilizing interface contacts (assumption (2)) that are neglected in Eqs. (1) and (2). Several reasons can be given for focusing our attention on the later possibility. First, *a priori* it would seem that a single Ala substitution at a solvent exposed position would have a negligible impact on the conformational integrity of an unbound monomer. Second, and not surprisingly, other groups have had excellent success predicting the binding affinity effects of $X \rightarrow$ Ala and other interface mutations without explicitly modeling conformational changes in the unbound monomer [16–18]. Third, numerous interactions are indeed missing from Eq. (2) and our previous research suggests that while the terms explicitly represented in Eq. (2) might be sufficient for accurate native or wt binding affinity prediction, the consideration of additional terms and interactions, specifically electrostatic interactions, are probably required for accurate non-native and mutant binding affinity prediction. Fourth and finally, it is advisable to consider simpler explanations before considering more complicated ones.

With the above in mind, we hypothesize that the net electrostatic free energy contributions of interchain polar-charge, long range charge–charge, π–π, and cation–π interactions are essential to protein–protein recognition and that the neglect of these interactions or the assumption that they somehow cancel (assumption (2)) is the key to explaining the majority of the predictive failures generated using Eqs. (1) and (2).

4.3. Comparison with previous work

Using an all-atom, multi-term, re-parameterized, free energy function Kortemme and Baker studied a total of 380 alanine mutations and 233 interface mutations (according to a 4 Å interchain distance criterion) from a diverse set of 19 protein–protein complexes. The final function developed and tested by Korteeme et al., included individual and weighted attractive and repulsive van der Waals terms, side chain and main chain hydrogen bonding potentials, and a sophisticated implicit solvent model. The various adjustable parameters were optimized on a training set of 743 $X \rightarrow$ Ala monomeric proteins. The hydrogen bonding weights were further re-scaled to maximize agreement with experimentally determined relative $X \rightarrow$ Ala binding free energy changes. For all 380 mutants, Kortemme and Baker reported an average unsigned error of 0.83 kcal and success rates of 69% and 84% respectively, for predicting the stability changes associated with neutral and hot spot alanine substitutions. For the 233 interface mutants, they reported an average unsigned error of 1.06 kcal and success rates of 79% and 68%, respectively [17].

Moreira et al. reported on a fully atomistic MD (molecular dynamics) MM-GB/SA (molecular mechanics generalized born surface area) computational method for predicting relative binding free energy differences between wild-type and alanine mutated protein–protein complexes. The methodology was used to make predictions for 46 alanine mutants from 3 different complex types. Using a ≈1.3 kcal criterion for identifying successful predictions, Moreira et al. reported an overall success rate of 80% and an impressive hot spot prediction success

rate of 82% and reported excellent success at predicting the effect of charged residue mutations. To obtain these results, however, Moreira et al. had to employ physically plausible but nonetheless additional and adjustable amino acid-dependent internal dielectric parameters [18].

According to gross statistical measures of accuracy and success, our methodology compares favorably with the methods of Kortemme and Baker and Moreira et al. The advantage of our method is its relative simplicity, low computational cost and lack of reliance on additional fitted parameters. Moreover, our method has been used to successfully predict absolute experimental binding affinities and to accurately score and rank native and non-native protein–protein interactions. The advantage of the Kortemme and Baker and Moreira et al. protocols are their strong physical and theoretical bases and their explicit calculation of numerous important interactions that are missing from Eqs. (1) and (2). What is suggested by our work and the work of Moriera et al. and Kortemme et al. is the potential for a symbiotic relationship, where one method is used to supplement the other. Consider, for example, a high throughput alanine mutagenesis screening protocol that employs Eq. (2) as the primary target or scoring function and that employs the MD MM-GB/SA method of Moriera et al. to more rigorously evaluate the relative binding affinities of select complexes. Alternatively, it is hoped that an analysis and understanding of all three studies will stimulate and guide the development of a single, rigorous, generally valid, and computationally tractable method.

4.4. The possibility of a simpler method and other considerations

A simpler and equally or even more predictive version of Eq. (1) is a logical possibility. However, our goal was not to develop a method to quantitatively predict $X \rightarrow$ Ala stability changes. Rather, our goal is to develop a single, simple, fast, generally valid, physically, theoretically and mathematically plausible method for predicting native and non-native protein–protein binding affinities. According to our experience, a simpler version of Eq. (1) cannot satisfy this goal. Furthermore, the simplicity of Eq. (1) should not be underestimated. For example, by eliminating Lennard-Jones like terms thousands of atomic interactions are avoided with all the associated computational costs. Finally, the reader is referred to the supplemental material to access additional information regarding (1) the individual relative free energy contributions of all six descriptors and (2) an inter-correlation analysis of all six descriptors. This additional information, while helpful, does not affect the analysis and inferences of the present paper.

5. Conclusion

Within the theoretical framework of rigid-body association, a growing body of evidence suggests that the six terms characteristic of Eqs. (1) and (2) capture much of the underlying physics of native or wt protein–protein recognition. The results of the present study (79% predictive success rate) lend further support to this view. This, in turn, would seem to suggest that native state or wt protein–protein interfaces are optimized to ensure that the various interactions and contributions neglected in Eqs. (1) and (2) make a net free energy contribution to binding of ≈ 0 ($\Delta G_{\text{native,other}} \approx 0$) and that assumption (2) is a reasonable and useful approximation for native interfaces.

On the other hand, the results of previous docking-based research and the results presented here, in particular for charged and aromatic residue mutations (mut), also suggest that as protein–protein interfaces become increasingly non-native, complexes are destabilized and the explanatory and predictive power of Eqs. (1) and (2) deteriorates. Presumably, this is because as protein interfaces take on an increasingly non-native character, through mutation or docking decoy generation, key interface contacts are disrupted or lost, assumption (2) breaks down, and $\Delta G_{\text{non-native,other}} > 0$. This possibility is currently neglected or assumed away in Eqs. (1) and (2). The evidence presented here and the results of our previous work suggest that these key interactions are electrostatic in nature and that non-native or mutant complex destabilization probably involves an upset or perturbed balance between the electrostatic desolvation penalty and the formation of stabilizing interchain polar-charge, long range charge–charge and π-mediated interactions. Future work will focus on an iterative process of modifying and testing Eq. (1) along the lines suggested here.

Appendix A. Supplementary data

Supplementary data associated with this article can be found, in the online version, at doi:10.1016/j.bpc.2009.05.003.

References

[1] Z. Liu, B.N. Dominy, E.I. Shakhnovich, Structural mining: self-consistent design on flexible protein–peptide docking and transferable binding affinity potential, J. Am. Chem. Soc. 126 (27) (2004) 8515–8528.
[2] J. Schymkowitz, et al., The FoldX web server: an online force field, Nucleic Acids Res. 33 (2005) W382–W388 (Web Server issue).
[3] C. Zhang, et al., A knowledge-based energy function for protein–ligand, protein–protein, and protein–DNA complexes, J. Med. Chem. 48 (7) (2005) 2325–2335.
[4] V. Zoete, M. Meuwly, M. Karplus, Study of the insulin dimerization: binding free energy calculations and per-residue free energy decomposition, Proteins 61 (1) (2005) 79–93.
[5] E.B. De Souza, et al., Novel therapeutic modalities to address nondrugable protein interaction targets, Neuropsychopharmacology 34 (1) (2009) 142–158.
[6] L. Gentilucci, A. Tolomelli, F. Squassabia, Peptides and peptidomimetics in medicine, surgery and biotechnology, Curr. Med. Chem. 13 (20) (2006) 2449–2466.
[7] D.P. McGregor, Discovering and improving novel peptide therapeutics, Curr. Opin. Pharmacol. 8 (5) (2008) 616–619.
[8] S.J. Projan, et al., Small molecules for small minds? The case for biologic pharmaceuticals, Expert Opin. Biol. Ther. 4 (8) (2004) 1345–1350.
[9] V. Rajakrishnan, V.R. Manoj, G. Subba Rao, Computer-aided, rational design of a potent and selective small peptide inhibitor of cyclooxygenase 2 (COX2), J. Biomol. Struct. Dyn. 25 (5) (2008) 535–542.
[10] M. Rubinstein, M.Y. Niv, Peptidic modulators of protein–protein interactions: progress and challenges in computational design, Biopolymers (2009).
[11] L.O. Sillerud, R.S. Larson, Design and structure of peptide and peptidomimetic antagonists of protein–protein interaction, Curr. Protein Pept. Sci. 6 (2) (2005) 151–169.
[12] Y. Yagi, et al., In silico panning for a non-competitive peptide inhibitor, BMC Bioinformatics 8 (2007) 11.
[13] J. Audie, S. Scarlata, A novel empirical free energy function that explains and predicts protein–protein binding affinities, Biophys. Chemist. 129 (2–3) (2007) 198–211.
[14] D.W. Ritchie, D. Kozakov, S. Vajda, Accelerating and focusing protein–protein docking correlations using multi-dimensional rotational FFT generating functions, Bioinformatics 24 (17) (2008) 1865–1873.
[15] J. Audie, Development and validation of an empirical free energy function for calculating protein–protein binding free energy surfaces, Biophys. Chemist. 139 (2–3) (2009) 84–91.
[16] R. Guerois, J.E. Nielsen, L. Serrano, Predicting changes in the stability of proteins and protein complexes: a study of more than 1000 mutations, J. Mol. Biol. 320 (2) (2002) 369–387.
[17] T. Kortemme, D. Baker, A simple physical model for binding energy hot spots in protein–protein complexes, Proc. Natl. Acad. Sci. U. S. A. 99 (22) (2002) 14116–14121.
[18] I.S. Moreira, P.A. Fernandes, M.J. Ramos, Computational alanine scanning mutagenesis—an improved methodological approach, J. Comput. Chem. 28 (3) (2007) 644–654.
[19] SloanD.J. , H.W. Hellinga, Dissection of the protein G B1 domain binding site for human IgG Fc fragment, Protein Sci. 8 (8) (1999) 1643–1648.
[20] ThornK.S. , A.A. Bogan, ASEdb: a database of alanine mutations and their effects on the free energy of binding in protein interactions, Bioinformatics 17 (3) (2001) 284–285.